IOP Publishing | Bureau International des Poids et Mesures Metrologia

Metrologia 52 (2015) S217–S226 doi:10.1088/0026-1394/52/5/S217

Dielectric-constant gas thermometry

Christof Gaiser, Thorsten Zandt and Bernd Fellmuth

Physikalisch-Technische Bundesanstalt (PTB), Abbestrasse 2–12, 10587 Berlin, Germany

E-mail: christof.gaiser@ptb.de

Received 19 December 2014, revised 20 February 2015
Accepted for publication 17 March 2015
Published 19 August 2015

Abstract

The principles, techniques and results from dielectric-constant gas thermometry (DCGT) are reviewed. Primary DCGT with helium has been used for measuring T–T_{90} below the triple point of water (TPW), where T is the thermodynamic temperature and T_{90} is the temperature on the international temperature scale of 1990 (ITS-90), and, in an inverse regime with T as input quantity, for determining the Boltzmann constant at the TPW. Furthermore, DCGT allows the determination of several important material properties including the polarizability of neon and argon as well as the virial coefficients of helium, neon, and argon. With interpolating DCGT (IDCGT), the ITS-90 has been approximated in the temperature range from 4 K to 25 K. An overview and uncertainty budget for each of these applications of DCGT is provided, accompanied by corroborating evidence from the literature or, for IDCGT, a CIPM key comparison.

Keywords: thermometry, dielectric constant, Boltzmann constant, polarizability, viral coefficients

(Some figures may appear in colour only in the online journal)

1. Introduction

The dielectric-constant gas thermometry (DCGT) developed in the 1970's in the U K [1, 2], and later improved by Physikalisch-Technische Bundesanstalt [3–7], is now a well established method of primary thermometry. Except for pressure measurement, DCGT has sources of error, which are quite different from those of other primary-thermometry methods based on the thermal equation of state of ideal gases [8]. Compared with the classical constant-volume gas thermometry, it has the advantage that the gas density is measured *in-situ* via the dielectric constant. Thus, DCGT does not require knowledge of the number of moles present in the gas bulb.

The paper reviews the principles, techniques and results from DCGT. In section 2, working equations for the evaluation of isotherm measurements are derived from basic statistical equations for a real gas. These working equations allow deduction of the ideal-gas behaviour by extrapolation to zero pressure. The experimental setup is described in section 3, and a general uncertainty budget is presented in section 4. In the following sections, the application of DCGT is discussed for primary thermometry at low temperatures (section 5), the determination of gas properties (section 6), the determination of the Boltzmann constant at the triple point of water (section 7), and the interpolation between fixed-point temperatures in the range from 4 K to 25 K (section 8). Finally, conclusions and an outlook are given.

2. DCGT principle

2.1. Basic equations

The basic idea of DCGT is to replace the density in the state equation of a gas by the dielectric constant and to measure this constant by the capacitance changes of a capacitor filled with gas at different pressures and constant temperature (measurement of isotherms). If the gas particles do not interact (ideal gas), the working equation can be simply derived by combining the classical ideal-gas law and the Clausius–Mossotti equation.

For a real gas in a general formulation including electrical fields, both input equations are power series containing different virial coefficients [3]:

$$p = \frac{RT}{V}\left(1 + \frac{B^*}{V} + \frac{C^*}{V^2} + \ldots\right), \tag{1}$$

with

$$B^* = B - \frac{3A_\varepsilon b^* D^2}{2RT\varepsilon_0} \text{ and } C^* = C - \frac{3A_\varepsilon c^* D^2}{RT\varepsilon_0}, \quad (2)$$

and

$$\frac{\varepsilon_r - 1}{\varepsilon_r} = \frac{3A_\varepsilon}{V}\left(1 + \frac{b^*}{V} + \frac{c^*}{V^2} + \ldots\right). \quad (3)$$

In these equations p is the pressure, T the thermodynamic temperature, R the molar gas constant, V the molar volume, B and C the second (pair) and third (mainly triplet) density virial coefficients, b^* and c^* the second and third dielectric virial coefficients, A_ε the molar polarizability, ε_0 the electric constant, ε_r the relative dielectric constant, and D the electric displacement. The density virial coefficients describe the multi-particle interaction during mechanical scattering, whereas the dielectric virial coefficients consider the electrical multipole interaction. In conventional constant-volume gas thermometry, no electric fields exist ($D = 0$), i.e. $B^* = B$ and $C^* = C$. The electric terms in equations (2) are only theoretically important, because the integrability condition

$$\left(\frac{\partial p}{\partial D}\right)_V = \frac{D}{\varepsilon_0}\left[\frac{\partial V(\varepsilon_r - 1)/\varepsilon_r}{\partial V}\right], \quad (4)$$

resulting from Gibbs fundamental thermodynamic equations, is not fulfilled without them, but under the experimental conditions of DCGT they can be neglected. From (3) the virial expansion of the Clausius–Mossotti equation is obtained neglecting higher-order terms:

$$\frac{\varepsilon_r - 1}{\varepsilon_r + 2} = \frac{A_\varepsilon}{V}\left(1 + \frac{b}{V} + \frac{c}{V^2} + \ldots\right), \quad (5)$$

with

$$b = b^* + 2A_\varepsilon \text{ and } c = c^* + 4A_\varepsilon b^* + 4A_\varepsilon^2, \quad (6)$$

where b and c are the dielectric virial coefficients usually used for DCGT.

A combination of equations (1) and (5) eliminates the molar volume V (see following section). The dielectric constant can be determined by measurements of the capacitance $C(p)$ of a capacitor, which is filled between its electrodes with gas of pressure p, and of the capacitance $C(0)$ of the same capacitor at zero pressure. This works ideally only for a pressure-independent configuration of the capacitor. In practice, changes of the electrode geometry with pressure are unavoidable and have to be taken into account. Applying the formulas for the capacitance given in [9], it can be shown that for a capacitor, which consists of cylindrical inner and outer electrode, the pressure dependence is linear to a good approximation:

$$C(p) = \varepsilon_r C(0)\,(1 + \kappa_{\text{eff}} p), \quad (7)$$

even if the two electrode axes are eccentric and not parallel. Here κ_{eff} is an effective compressibility of the complete capacitor assembly. In a suitable design it is nearly equal to the linear compressibility of the electrode bulk material. However it is a system parameter, which has to be determined for each individual design.

DCGT can be used as a primary thermometer only if the molar polarizability A_ε contained in the Clausius–Mossotti equation (equation (5)) is known from fundamental principles or independent thermodynamic measurements with sufficient accuracy. A_ε is defined as $A_\varepsilon = N_A\alpha_0/(3\varepsilon_0)$, with N_A being the Avogadro constant and α_0 the static electric dipole polarizability of the gas particles. At present, a sufficiently accurate value for α_0, obtained from *ab initio* calculations, is available only for helium, providing a relative uncertainty below one part per million (1 ppm), are available [10–12]. The obtained value from [10] is in SI units $\alpha_0(^4\text{He}) = 2.2815133(4) \times 10^{-41}\,\text{C m}^2\,\text{V}^{-1}$ and has an uncertainty of 0.2 ppm. The *ab initio* calculations, usually performed in atomic units, yielded exactly the polarizability of the 1^1S ground state of the ^{4}He atom, $\alpha_0^*(^4\text{He})$, which is connected with $\alpha_0(^4\text{He})$ via the relation

$$\alpha_0(^4\text{He}) = 4\pi\varepsilon_0 a_0^3 \alpha_0^*(^4\text{He}), \quad (8)$$

where a_0 is the Bohr radius and ε_0 is the fixed electrical constant. With the fundamental constants published by CODATA in [13], from $\alpha_0^*(^4\text{He})$ given in [10] and its uncertainty one obtains $A_\varepsilon(^4\text{He}) = 5.1725413(9) \times 10^{-7}\,\text{m}^3\,\text{mol}^{-1}$.

2.2. Working equation for low temperatures

The derivation of a DCGT working equation requires to combine the two power series equation (1) with $B^* = B$ and $C^* = C$ and equation (5) with ε_r determined from capacitance measurements corresponding to equation (7). At temperatures below about 50 K, the influence of the gas pressure on the capacitor dimensions is sufficiently described by using the lowest order with respect to κ_{eff} in the power expansion of the combination of the two series. Using the observable relative capacitance change

$$\gamma = \frac{(C(p) - C(0))}{C(0)} = \varepsilon_r - 1 + \varepsilon_r \kappa_{\text{eff}}\, p \quad (9)$$

and the substitution $\mu = \gamma/(\gamma + 3)$, the combination yields in this approximation and neglecting higher-order terms the following power expansion for the pressure p at a fixed temperature T

$$p = A_1\mu(1 + A_2\mu + A_3\mu^2 + \ldots), \quad (10)$$

with the coefficients

$$A_1 = (A_\varepsilon/(RT) + \kappa_{\text{eff}}/3)^{-1}, \quad (11)$$

$$A_2 = (B(T) - b(T))/A_\varepsilon, \quad (12)$$

$$A_3 \approx C(T)/A_\varepsilon^2. \quad (13)$$

This equation was the basis for the DCGT measurements described e.g. in [1, 3, 14, 15]. The coefficients A_1, A_2, and A_3 can be determined by fitting to a sufficient number of data pairs (p_i, μ_i) $(i = 1, 2, \ldots, n)$ obtained at the same temperature. For such a single-isotherm fit (SIF), the thermodynamic temperature can be deduced from A_1 via equation (11). But as shown in [16], an enormous decrease of the uncertainty is

achieved if the experimental data for a large number of isotherms are fitted together applying appropriate series for the temperature dependencies of the virial coefficients, e.g.

$$B(T) - b(T) = \sum_j B_j T^j, \tag{14}$$

$$C(T) = \sum_k C_k T^k. \tag{15}$$

By inserting equations (11)–(15) in equation (10), while using for equation (11) the approximation

$$A_l = \frac{R}{A_e}(T_S + \Delta T_S) - \frac{\kappa_{eff}}{3}\left(\frac{RT_S}{A_e}\right)^2, \tag{16}$$

one obtains if terms with products of κ_{eff} and the virial coefficients are neglected

$$p - \frac{R}{A_e}\Delta T_S\,\mu = \frac{R}{A_e}T_S\,\mu - \frac{\kappa_{eff}}{3}\left(\frac{R}{A_e}\right)^2 T_S^2\mu + \frac{RT_S}{A_e^2}\sum_j B_j T_S^j \mu^2 + \frac{RT_S}{A_e^3}\sum_k C_k T_S^k \mu^3, \tag{17}$$

where $\Delta T_S = T_{DCGT} - T_S$. Here, T_{DCGT} is the temperature determined by DCGT, and T_S is the temperature measured with a thermometer carrying some practical scale. Equation (17) is linear in the functions of the argument μ. Omitting the second term on the left-hand side for the time being, it can be fitted by a least-square method to all pairs (p_{il}, μ_{il}) to get the coefficients B_j and C_k with $l = 1, 2, ..., q$ (q number of isotherms) and $i = 1, 2, ..., n_l$ (n_l number of measurements on the isotherm l). But this multi-isotherm fit (MIF) is not a true surface fit because only μ is the fit variable. An information on temperature, being the second variable in a triplet (p_{il}, T_{Sl}, μ_{il}), can be deduced only via the determination of correction ΔT_{Sl} on the left-hand side of (17) from the fit residuals. This has to be done by an iteration procedure assuming an equal value ΔT_{Sl} for all measurements on a single isotherm. The iteration starts with $\Delta T_{Sl} = 0$. Then the ΔT_{Sl} are recalculated step by step and added to the isotherm temperatures $T_{Sl,start}$, used for the first iteration step, ($T_{Sl} = T_{Sl,start} + \Delta T_{Sl}$) to improve the fit until convergence is reached at the desired uncertainty level. It should be emphasized that the particular choice of the $T_{Sl,start}$ has no influence on the results at the end of the iteration. The application of equation (17) decreases very powerful the uncertainty because the complete ensemble of experimental data is used for one fit.

2.3. Extended working equation

For temperatures above about 50 K, including measurements near the TPW, the determination of the virial coefficients requires higher orders to be considered in the working equation compared with the low-temperature one. (This extension has no effect on the results for the determination of the thermodynamic temperature T or the Boltzmann constant k, which are deduced from the linear ideal-gas term of the working equation.) Considering terms up to the fourth virial coefficients, the virial expansions are given by

$$p = \frac{RT}{V}\left(1 + \frac{B}{V} + \frac{C}{V^2} + \frac{D}{V^3}\right) \tag{18}$$

and

$$\frac{\varepsilon_r - 1}{\varepsilon_r + 2} = \frac{A_\varepsilon}{V}\left(1 + \frac{b}{V} + \frac{c}{V^2} + \frac{d}{V^3}\right). \tag{19}$$

Again, the working equation should allow a fit of the measured DCGT isotherms with a linear series expansion, and it should not contain the volume V. Using the two abbreviations

$$x = \frac{b}{V} + \frac{c}{V^2} + \frac{d}{V^3} \text{ and } y = \frac{\varepsilon_r - 1}{\varepsilon_r + 2}$$

Equations (18) and (19) can be rearranged as follows:

$$p = RT\left[\frac{1}{\left(\frac{A_\varepsilon}{y}(1+x)\right)} + \frac{B}{\left(\frac{A_\varepsilon}{y}(1+x)\right)^2} + \frac{C}{\left(\frac{A_\varepsilon}{y}(1+x)\right)^3} + \frac{D}{\left(\frac{A_\varepsilon}{y}(1+x)\right)^4}\right] \tag{20}$$

and

$$(1+x) = \left[1 + \frac{b}{\left(\frac{A_\varepsilon}{y}(1+x)\right)} + \frac{c}{\left(\frac{A_\varepsilon}{y}(1+x)\right)^2} + \frac{d}{\left(\frac{A_\varepsilon}{y}(1+x)\right)^3}\right]. \tag{21}$$

To find a linear approximation of the problem, the terms containing x in the denominator are expanded applying the binomial series. In view of the smallness of the dielectric virial coefficients, this is done first for equation (21) considering only the first expansion terms. A rearrangement and a further expansion of the result yields x as a function of A_ε, y, b, c, d, i.e. the volume V is removed as necessary. The derived expression for $x(A_\varepsilon, y, b, c, d)$ is inserted in equation (20), which is expanded considering the first and second expansion terms. Then the theoretical working equation is obtained taking into account only terms up to order four in y.

For the quantity μ, which is equal to y for $\kappa_{eff} = 0$, it follows from equation (9):

$$\mu = 1 + \frac{3(y-1)}{3 + \kappa_{eff}p(1+2y)}. \tag{22}$$

Replacing in the small correction term $\kappa_{eff}\,p(1+2y)$ the pressure p by yRT/A_ε and the ratio y by μ yields

$$y = \frac{\mu}{1 + \frac{\kappa_{eff}RT}{3A_\varepsilon} + \frac{\kappa_{eff}RT}{3A_\varepsilon}(\mu - 2\mu^2)}. \tag{23}$$

which can be expanded with the result

$$y = \frac{\mu}{1 + \frac{\kappa_{eff}RT}{3A_\varepsilon}} - \frac{\mu(\mu - 2\mu^2)\frac{\kappa_{eff}RT}{3A_\varepsilon}}{\left(1 + \frac{\kappa_{eff}RT}{3A_\varepsilon}\right)^2}. \tag{24}$$

Insertion of equation (24) in the theoretical working equation leads with equation (11) to

$$p = A_1\mu\left(\begin{array}{l} 1+\mu A_1\left(\frac{1}{RT}(B-b)-\frac{\kappa_{\rm eff}}{3}\right)+\mu^2A_1^2\left\{\left(\frac{1}{RT}\right)^2(C-2Bb+2b^2-c)+\frac{2\kappa_{\rm eff}}{3A_1}+\frac{2\kappa_{\rm eff}}{3RT}(b-B)\right\} \\ +\mu^3A_1^3\left\{\begin{array}{l}\left(\frac{1}{RT}\right)^3[D-d-3bC-2Bc+5bc+5b^2B-2b^3]- \\ \left(\frac{1}{RT}\right)^2\kappa_{\rm eff}[-2Bb+2b^2+C-c]+\frac{1}{RT}\left(\frac{\kappa_{\rm eff}}{3}\right)^2(B-b)+\left(\frac{4\kappa_{\rm eff}}{3RTA_1}\right)(B-b)\end{array}\right\}\end{array}\right) \tag{25}$$

The terms with the factor $1/RT$ in second and $(1/RT)^2$ in third order are similar to those taken into account in [1], but with the difference that in equation (25) the higher-order terms are multiplied by powers of A_1. This facilitates better consideration of the effects of compressibility. In the approach, which was sufficient for measurements at low temperatures, all higher-order terms were simply multiplied by A_1, see section 2.2. As a rule of thumbs, following from equation (11), the impact of $\kappa_{\rm eff}$ and higher order terms decreases with increasing polarizability and decreasing temperature.

3. Experimental setup

3.1. Measuring capacitors

Though toroidal (ring) cross capacitors may have advantages [17, 18], up to now all groups have used cylindrical measuring capacitors for DCGT [1, 2, 6, 15, 19]. As described in [5], in an ideal cylindrical capacitor design, only the relative change $\Delta l(p)/l(p=0)$ of the electrode length l is relevant, i.e. $\kappa_{\rm eff}$ is one third of the volume compressibility of the electrode material, which is the inverse of the bulk modulus. This elastic property can be determined with resonant ultrasound spectroscopy (RUS) [20, 21], which uses normal-mode resonance frequencies of free vibration as well as data on the shape and the mass of the sample. But it has to be considered that the compressibility measured by RUS is the adiabatic one, whereas for the DCGT the isothermal compressibility is needed. For the conversion from the adiabatic $\kappa_{\rm ad}$ to the isothermal value $\kappa_{\rm iso}$, Grüneisen has derived the relation $\kappa_{\rm iso} = \kappa_{\rm ad} + TV_{\rm m}\alpha_V{}^2/C_p$ [22], with the molar volume V_m, the thermal-expansion coefficient α_V and the molar specific heat capacity C_p at constant pressure.

The effective compressibility may also be influenced by an eccentricity of the capacitor electrodes and an eccentric tilt as well as the change in stray capacitances and a relative displacement of the electrodes under pressure. Furthermore, in reality, a rigid capacitor is a complicated geometrical object because electrically isolating pieces and stabilizing screws are necessary. Thus, the isothermal compressibility of a composite has to be determined. Using tungsten carbide (electrodes) and aluminium oxide (isolating discs) as construction materials, for the design described in [19], a relative standard uncertainty of 0.17% was achieved at the TPW, as reported in [6]. This was possible by checking the mounting of the electrodes applying a coordinate measuring machine. In addition, simulations with the finite-element method regarding the influences of the relative displacement of the electrodes and stray capacitances have been performed.

3.2. Temperature control and measurement

Both at low temperatures and near to the TPW, the temperature can be controlled well within one tenth of a millikelvin under steady-state conditions over long time periods of weeks if (i) all thermometers are thermally anchored to a central copper piece with high thermal conductivity and (ii) this measuring assembly is surrounded by an isothermal shield and placed within a vacuum can for thermal isolation [4, 14, 18, 23]. Furthermore, the uncertainty component due to static temperature-measurement errors can be decreased to the same sufficient level. Using capsule-type platinum or rhodium–iron resistance thermometers and commercial resistance measuring bridges calibrated traceably to the national standards, the overall uncertainty of the temperature measurement with respect to ITS-90 or the TPW temperature can reach an order of a few tenth of a millikelvin [6, 14, 24].

Special problems are caused by unavoidable features of the DCGT experimental setup. During the experiments, the temperature of the capacitor electrodes inside the pressure vessels cannot be measured directly. It is not possible to place thermometers inside the vessels because of the requirement to guarantee a high purity of the measuring gas. During such measurements, the flow of the measuring gas for changing the pressure inside the pressure vessel causes warming or cooling and thus temporary temperature changes. It is, therefore, necessary to investigate the thermal recovery of the system in order to reduce dynamic temperature-measurement errors. Such investigations were especially performed for a huge measuring system with a very slow thermal recovery due to its large mass and thus heat capacity [18, 23]. This system was used for the determination of the Boltzmann constant at the TPW [5, 6], see section 7. Dedicated experiments have been performed by simulating the gas-flow-induced temperature changes via the application of heat pulses. The experimental results have been compared with theoretical calculations based both on simple rough models and finite-element methods. The investigations yielded an agreement between experiment and theory, which is sufficient for deducing the temperature of the capacitor electrodes inside the pressure vessels with an uncertainty of order one tenth of a millikelvin. Under the real experimental conditions, this theoretical description of the recovery is of course accompanied by a careful observation of the drift of the capacitance values with time.

3.3. Capacitance measurement

Helium is the only measuring gas, the polarizability of which can be calculated theoretically with the necessary relative

uncertainty well below 1 ppm, see section 2.1. But the polarizability of helium is very small. To give an example, at a pressure of 0.1 MPa and at the TPW, the electric susceptibility of helium has only a value of 7×10^{-5}. Though pressures up to 7 MPa are used in [5, 6], a high-resolution and high-precision bridge is needed that allows to measure small capacitance changes of at most a few 0.1% with a relative standard uncertainty below 1 ppm, i.e. with an uncertainty relative to the capacitance value of order (one part per billion) 1 ppb.

These extreme demands cannot be fulfilled with commercial capacitance measurement equipment. Therefore, at PTB two quite different custom-made bridges are used for measuring the relative capacitance changes, namely a bridge circuit based on a nine-decade high-precision inductive voltage divider (IVD) [3] and an autotransformer ratio capacitance bridge with a high-precision 1:1 IVD and current injection [25]. The uncertainty estimates presented in [25] show that the necessary uncertainty can be obtained only because the measurements of $C(p)$ and $C(0)$, to be inserted in equation (9), are correlated and the measuring circuit is fully symmetric. (As sketched in figure 1, the reference capacitor is also located in the measuring system within the vacuum chamber.) Within the upper ratio-error limits of the nine-decade IVD of 10 ppb, no discrepancies have been found between the two home-made bridges.

The bridges are not applied under ideal measuring conditions because the capacitors have to be placed within a cryostat or a thermostat. This causes large parasitic impedances due to, e.g. long measuring coaxial cables and non-ideal connections to the reference point of the network. For each experiment, it is necessary to optimise the capacitance measurement testing the individual conditions, see [6, 14, 26] for details. This concerns especially (i) the reduction of the interference induced by external magnetic fluxes based on a careful analysis of the network as recommended in [27], and (ii) the improvement of the resolution by decreasing the parasitic capacitance to ground, using low-noise cables, and narrowing the bandwidth. At all pressures, capacitance measurements were performed for the two opposite connections of the high-level terminals of the measuring and reference capacitors to the bridge. This yields information on the Type B uncertainty component of the inductive voltage divider and the consistency of the data. Furthermore, it increases the additional, statistical information on the errors of the IVD decades used for balancing the bridge (Type A uncertainty component).

3.4. Gas-handling system and purity analysis

The highest requirements regarding the purity of the measuring gas result from the determination of the Boltzmann constant at the TPW using helium. Impurities should not cause a relative change of the result by more than 1 ppm. To prevent contamination of the helium of nominal purity 99.99999% during handling, the gas purifier (adsorber) Micro Torr SP70 from SAES Pure Gas, Inc., and the helium purifier (getter) HP2 from Valco Instruments, Co. Inc., have been incorporated in the ultra-high-purity gas-handling system described in [5, 6] [1]. (For the getter, the specified upper limit for water and the other relevant impurities beside noble gases is 10 parts per billion. For the adsorber, the specified upper limit for water and the other relevant impurities beside noble gases is 0.1 parts per billion.) After each measurement of an isotherm, which lasted usually one week, the measuring gas was analysed with the aid of a mass spectrometer (GAM 400, InProcess Instruments) to check for a possible contamination especially due to outgassing from the different pieces inside the pressure vessel. The analysis has been developed further by evaluating the spectra absolutely (without the self correction of the spectrometer) and removing the background (noise and other parasitic signals) more efficient by frequent switching between measuring gas from the capacitor and original gas from the supplied bottle. The detection limit for noble gas contaminations is 10 ppb. The most problematic impurity is water because it has a polarizability 160 times larger than that of helium. Thus, the detection limit of 20 parts per billion would cause an uncertainty component of order 1 ppm applying a rectangular distribution. But considering the specification of the adsorber 1 ppm seems to be a reliable upper estimate for an overall uncertainty component including all relevant impurities.

3.5. Pressure measurement

The requirements regarding absolute pressure measurements are quite different for the various application fields of DCGT. This ranges from measuring pressures down to about 0.01 MPa with a relative uncertainty of order 10 ppm (primary thermometry down to about 2.5 K) to measuring pressures up to 7 MPa with a relative uncertainty of order 1 ppm (determination of the Boltzmann constant at the TPW). These requirements can be fulfilled only by using pressure balances, which act moreover as pressure stabiliser. For the second goal, it was necessary to characterise pressure balances with an unprecedented quality and even to improve the national standard of PTB significantly. A system of special pressure balances, as outlined in [28, 29], was designed, constructed and evaluated [30–33], see also the summary in [5]. The system includes two pressure-balance platforms, three piston-cylinder units (PCUs) with effective areas of 20 cm^2 and three 2 cm^2 PCUs. Traceability to the SI base units up to 7 MPa was realised in two steps. First, the zero pressure effective areas of the 20 cm^2 PCUs have been determined from dimensional measurements. Second, the 2 cm^2 PCUs have been calibrated against the 20 cm^2 PCUs by cross-float comparisons. The calibration of the mass pieces traceable to the national mass standards and the accurate determination of the local gravity acceleration did not cause special challenges.

For the pressure measurement between about 0.01 MPa and 0.3 MPa two pressure balances with 3 cm^2 PCUs were calibrated traceably to the national standard of PTB with a relative uncertainty of 5 ppm. In 1996, the calibration was performed against a mercury manometer. The stability has been

[1] Identification of commercial equipment and materials in this paper does not imply recommendation or endorsement by PTB, nor does it imply that the equipment and materials identified are necessarily the best available for the purpose.

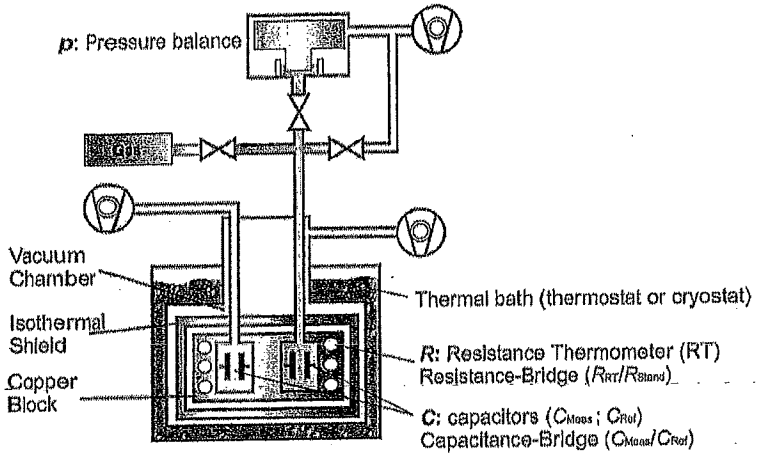

Figure 1. Schematic sketch of the DCGT setup used at PTB (reference capacitor C_{Ref} on the left, measuring capacitor C_{Meas} on the right). Three quantities have to be measured: pressure p, capacitance ratio leading to the quantity μ and resistance ratio leading to temperature T_S via the calibrated thermometer resistance R_{RT} and a calibrated standard resistor R_{Stand}.

verified by cross-floating measurements with the two systems in 2004 [26] and with the 20 cm^2 PCUs mentioned above in 2014.

The *in-situ* measurement of the gas density in DCGT allows to make the inner diameter of the pressure sensing tubes so large that the thermomolecular pressure difference between the gas bulb at the measuring temperature and the pressure sensor at room temperature is negligible even at the lowest temperatures and pressures. Thus, a correction considering this effect is not necessary. But another correction has to be applied very carefully, namely the so-called aerostatic head correction caused by the pressure difference produced by the gas columns between the bulb and the sensor. For calculating the head correction, the temperature along the tubes has to be controlled and measured. Its uncertainty can be ultimately decreased by isolating the tubes thermally, e.g. by leading them through vacuum, and concentrating temperature gradients at horizontal tube pieces. Taking these measures, the resulting uncertainty component could be reduced below 10 ppm both for helium at 2.4 K [14] and neon at 23 K and above [15]. Here the contribution of the tube pieces at low temperatures is largest due to the high gas density. Thermal isolation and controlling of the temperature along the whole tubes is also important for the stability of the pressure distribution and thus the DCGT measurement in general [6].

4. Uncertainty budgets

For all DCGT results obtained at PTB, uncertainty budgets have been established in accordance with the *Guide to the Expression of Uncertainty in Measurement* [34], see [3–6, 14, 15, 24, 35]. Some of these uncertainty budgets are also given in sections 5 to 8. The relevant components are listed in table 1 together with some comments. The direct access to the uncertainty estimates is hindered because the final result (T or A_e/R) is contained in the parameter A_1, see equation (11), which is gained by fitting (SIFs or even MIFs). Therefore, the statistical information for estimating the type A components has been deduced by Monte-Carlo simulations (MCSs). Fortunately, this allows also consideration of the pressure dependence of the uncertainty sources. The simulations can be performed with data sets randomized with the standard deviation of the specific quantity. Furthermore, the combined type A estimate can often be corroborated by the comparison of the results obtained applying different fits. The type B components consider uncertainty sources, which influence the result systematically.

The first seven components are already discussed in the sections specified in the second column. The component caused by impurity surface layers (dielectric films) is usually very small if the layers are stable between the measurement of $C(p)$ and $C(0)$. The influence of layers of the measuring gas is more complicated because it is dependent on pressure. Its treatment requires investigation of the difference between $C(0)$ values obtained immediately before and after an isotherm measurement and to consider literature data on the number of mono-layers covering the capacitor electrodes in dependence on pressure (adsorption isotherms) [14]. The last two uncertainty components listed in table 1 are specific for primary and interpolating thermometry, respectively, over extended temperature ranges. For the determination of thermophysical properties of the measuring gas, only a subset of components is relevant, see section 6.

5. Primary thermometry at low temperatures

Primary DCGT data has been obtained at PTB with two quite different apparatuses. Only the bridge circuit based on a nine-decade high-precision IVD, see section 3.3, was used in both measurement campaigns. The obtained data sets are called DCGT1 (228 triplets (p_{il}, T_l, μ_{il}) in the temperature range from 4.2 K to 27 K), published graphically in [3], and DCGT2 (174 triplets (p_{il}, T_l, μ_{il}) from 3.7 K to 27 K), published in its entirety as a table in [4]. Both data sets have been evaluated applying linear least-squares MIFs with equation (17) and orthogonal functions [36]. Data set DCGT2 was combined

Table 1. Overview of the components of uncertainty budgets for DCGT results.

Component	Comments
Susceptibility measurement (capacitance change)	Type A and B, capacitor and bridge, see sections 3.1 and 3.3
Determination of effective compressibility	Type B, RUS, FEM, see section 3.1
Pressure measurement	Type A and B, see section 3.5
Head correction (pressure of gas columns)	Type B, see section 3.5
Temperature measurement	Type A and B (traceability to the TPW or to fixed-point temperatures for IDCGT), see section 3.2
Impurities (measuring gas)	Type B, see section 3.4
Polarizability (measuring gas)	*Ab initio* calculation (He) or experiment, see section 2.1
Surface layers (impurities)	Type B
Surface layers (measuring gas)	Type B
Influence of temperature expansions for the virial coefficients like equations (14) and (15)	Type B for MIFs
Deviation from ideal gas law	Type B, IDCGT

with additional data down to 2.4 K in [24], and up to 36 K in [15]. In the latter paper, results obtained with ^{3}He and Ne as measuring gases are also discussed. The ^{3}He data and additional data for ^{4}He at 84 K (triple point of Ar), 120 K, 130 K, and 140 K, to be published elsewhere [37], were treated performing SIFs.

The DCGT setup applied for determining data set DCGT2 is described extensively in [24], and in full detail in [14]. The main improvements compared with the setup used in [3] are (i) a better temperature stability and homogeneity, (ii) an improved capacitance measurement due to an inclusion of the reference capacitor inside the cryostat (symmetric capacitance-bridge circuit) and averaging over long periods in view of the good temperature stability, and (iii) a smaller uncertainty of pressure measurement due to a better calibration of the pressure balances and more reliable p corrections. These improvements besides others lead to a reduction in the uncertainty of T_{DCGT} by a factor of two compared with [3]. As an example, table 2 shows the uncertainty budget established in [14, 24]. The seventh component listed in table 1 is here smaller than 0.01 mK, and the last component is not applicable.

For evaluating the data and estimating the uncertainty components, different methods were applied. The main variations are as follows:

5.1. Determination of the effective compressibility

Until 2010, the effective compressibility was deduced from DCGT measurements at the triple point of Ar assuming that the temperature value T_{90}(Ar) = 83.8058 K, which is defined for this fixed point in the text of the ITS-90, sufficiently approximates the thermodynamic one. The temperature dependence of κ_{eff} is so small that it could be considered as additional uncertainty component. Later on it became clear that T_{90}(Ar) is above the thermodynamic scale by (2–3) mK [37, 38]. To have a self-consistent determination of κ_{eff}, a new methodology has been developed [37, 39]. It starts with DCGT measurements at the TPW and RUS results between 230 K and 330 K, and utilises the relationship between the thermal expansion and the temperature dependence of the compressibility of solids that was first derived by Grüneisen [40] applying fundamental thermodynamic relations and making reasonable phenomenological approximations. The thermal expansion can be measured *in-situ* via the resulting change of the capacitance of the cylindrical capacitors. The methodology has been checked by comparison with literature data, e.g. for Cu.

Table 2. Uncertainty budget for three temperature values resulting from a multi-isotherm fit (MIF) to DCGT data (the uncertainty estimates for the different expansions for the temperature dependence of the virial coefficients (equations (14) and (15)) are practically the same, i.e. only one budget is necessary for each temperature). The estimates are given in mK.

Component	2.4 K	12 K	26 K
Monte-Carlo simulations (type A components) [a]			
Susceptibility measurement (capacitance change)	0.03	0.07	0.14
Pressure repeatability	0.03	0.02	0.03
Temperature instability	0.02	0.03	0.06
^{4}He layers	0.12	0.15	0.19
Effective compressibility	0.01	0.03	0.16
Type B estimates [b]			
Pressure (effective area)	0.01	0.06	0.13
Impurity layers	0.01	0.02	0.04
Impurities in the gas	0.01	0.04	0.07
Head correction	0.02	0.03	0.03
Influence of expansions for the virial coefficients [c]			
Temperature expansions	0.01	0.03	0.23
Combined standard uncertainty	**0.13**	**0.19**	**0.40**

[a] These uncertainties are based on Monte-Carlo simulations performed with one hundred data sets randomized with the standard deviation of the specific quantity.
[b] These uncertainties are based on calibrations and comparisons of pressure balances for determining the effective area, on literature data for the typical thickness of impurity layers on the capacitor plates, and analysis data (mass spectroscopy) for impurity concentrations in the measuring gas.
[c] This uncertainty component considers the deviations between the results obtained for the different expansions for the temperature dependence of the virial coefficients.

5.2. Expansions for the temperature dependence of the virial coefficients

Data set DCGT1 has been evaluated in [3] and [41] using different expansions for the temperature dependence of the virial

coefficients. For data set DCGT2, several different expansions have been tested, too. But only the most recent ones, presented in [4], have a complete theoretical basis [42, 43]:

$$B(T) = b_1 + b_2T^{-1.5} + b_3T^{-1} + b_4T, \quad (26)$$

$$C(T) = c_1 + c_2T^{-3} + c_3T^{-2} + c_4T^{-1.5}. \quad (27)$$

These expansions have been used in [15] for $B(T)$—$b(T)$ and $C(T)$, respectively, cf. equations (14) and (15).

5.3. Estimation of the uncertainty of the MIFs

The quality of the MIFs was evaluated in [3] applying three statistical criteria. One was the variance of the data calculated from their deviations from the fit functions. But the three criteria did not allow selecting one best fit. All acceptable fits were called 'best fits', and the uncertainty of the fit results was mainly estimated from the maximum difference between the 'best fits'. Another way was used since 2008 [14, 15, 24]: For obtaining statistical information, Monte-Carlo simulations have been performed. Here the input quantities are randomised, where the variation of the random numbers corresponds to the level of the uncertainty estimated for the specific quantity.

5.4. Estimation of the influence of surface layers

The maximum possible influence of stable surface layer was estimated in [3] by comparing the results obtained with two measuring capacitors, the history and handling of which were quite different. The effects due to films of condensed impurities and helium were treated considering the investigations in [1, 44]. Alternatively, the influence of layers of the measuring gas was corrected for in [14, 24] (Helium) and [15] (neon). In each case, the correction was based on two measurements of $C(0)$ (before and after the measurement of $C(p)$) and literature data on adsorption isotherms.

The differences between the results of the various evaluations are always within the estimated uncertainties. The DCGT scales were first of all compared with the constant-volume gas-thermometry scale NPL-75 [45] of the National Physical Laboratory, UK, being one of the bases of the ITS-90. The NPL-75 has been supported by later measurements as the best thermodynamic [38]. Thus, the coincidence of the DCGT scales with the NPL-75 within the uncertainty limits corroborates the usefulness of DCGT for primary thermometry.

6. Determination of gas properties

Applying SIFs with equations (10) or (25) and/or MIFs with equation (17), the following thermophysical properties have been determined with DCGT (the measurement temperatures are given in brackets):

(a) Polarizability:
^{3}He [46] (2.5 K, 3.2 K), Ne [35, 47] (26 K–36 K, 84 K, 120 K, TPW), Ar [47] (TPW);

(b) Virial coefficients:
^{3}He [46] (2.5 K, 3.2 K), ^{4}He [3, 4, 7, 14, 15, 24, 41, 47] (2.4 K–36 K, 84 K, 120 K, 130 K, 140 K, TPW), Ne [47] (23 K–36 K, 84 K, 120 K, TPW), Ar [47] (TPW).

According to equations (12) and (25), the determination of the density virial coefficients requires data on the dielectric virial coefficients. As discussed in section 5, different methods were applied for evaluating the data and estimating the uncertainty. Both for the polarizability values and those of the virial coefficients, the comparison with literature data corroborates the usefulness of DCGT as a tool for investigating the thermophysical properties of gases.

Because the polarizability of ^{4}He is known with the very small relative uncertainty of only 0.2 ppm from *ab initio* calculations, cf. section 2.1, a simple way was used in [35] for determining the polarizability of Ne. Isotherms were measured with ^{4}He and Ne at the same temperature T. Fits of the two sets of data with equation (10) yielded the coefficient $A_1(T)$ for both gases, i.e. a combination of both results by replacing the thermal energy RT contained in equation (11) leads to the relation

$$A_\varepsilon^{\mathrm{Ne}} = A_\varepsilon^{\mathrm{He}} \frac{A_\mathrm{l}^{\mathrm{He}}}{A_\mathrm{l}^{\mathrm{Ne}}} \left(\frac{A_\mathrm{l}^{\mathrm{Ne}} \kappa_{\mathrm{eff}} - 3}{A_\mathrm{l}^{\mathrm{He}} \kappa_{\mathrm{eff}} - 3} \right), \quad (28)$$

where the indices He and Ne denote the specific quantities. Due to the very small polarizability of ^{4}He, the experimental application of equation (28) places, however, extreme demands on the equipment used for measuring p, T, and μ.

For the uncertainty budgets of the virial coefficients, the Type B uncertainty components, like the effective area of the piston-cylinder assembly, lead to negligible contributions, whereas the Type A uncertainty components, like the temperature instability and the standard deviation of the capacitance measurement, contribute essentially to the combined uncertainty. Examples are given in [4].

7. Determination of the Boltzmann constant

The measurement of DCGT isotherms at a known thermodynamic temperature T allows determination of the ratio A_ε/R from the parameter A_1, which is contained in the expansions used for fitting the data (equations (10) or (25)) and given by equation (11). In turn this ratio yields the Boltzmann constant according to the relation

$$k = (\alpha_0/(3\varepsilon_0))/(A_\varepsilon/R), \quad (29)$$

and with equation (8) in atomic units $k = 4/3\ \pi\ \alpha_0^*(^4\mathrm{He})a_0^3 / (A_\varepsilon/R)$.

As applied in [5, 6], the easiest, absolute way for performing this determination of k by inverse primary thermometry is to do the measurements at the TPW because its thermodynamic temperature is defined to be $T_{\mathrm{TPW}} = 273.16$ K. But also a relative way is possible, if thermodynamic data are available away from the TPW [48].

For DCGT at the TPW, at PTB a special experimental setup has been developed [5, 6] that consists of

Table 3. Uncertainty budget for the determination of the Boltzmann constant k by dielectric-constant gas thermometry at the triple point of water in 2013.

Component	$u(k)/k \cdot 10^6$
Type A estimate	
Uncertainty of the overall weighted mean of A_1 values from 10 isotherms	2.6
Type B estimates	
Susceptibility measurement (capacitance change)	1
Determination of the effective compressibility κ_{eff}	2.4
Temperature (traceability to the TPW using capsule-type thermometers)	0.3
Pressure measurement (7 MPa)	1.0
Head correction (pressure of gas columns)	0.2
Impurities (measuring gas)	1
Surface layers (impurities)	0.5
Polarizability from *ab initio* calculation (theory for helium)	0.2
Combined standard uncertainty	**4.0**

- A large-volume thermostat containing a vacuum-isolated measuring system, the thermal conditions have been characterised in detail (section 3.2),
- Stainless-steel and tungsten carbide 10 pF cylindrical capacitors (section 3.1),
- An autotransformer ratio capacitance bridge (section 3.3),
- A high-purity gas-handling system including a mass spectrometer (section 3.4), and
- Traceably calibrated special pressure balances with piston-cylinder assemblies having effective areas of 2 cm^2 (section 3.5).

Progress concerning the design and the assembling of the measuring capacitor, the determination of its effective compressibility, the sensitivity of the capacitance bridge, the influence of stray capacitances, the purity of the measuring gas, the pressure measurement, and the scattering and the evaluation of the data has yielded a value of the Boltzmann constant of $k = 1.3806509 \times 10^{-23}\,J\,K^{-1}$. The uncertainty budget for this value is given in table 3.

The last three components listed in table 1 are here negligible or not applicable. Compared with the budget presented in [6] the estimate for the pressure measurement is reduced from 1.9 ppm to 1.0 ppm based on a reanalysis considering recently performed cross-floating experiments with the six piston-cylinder units mentioned in section 3.5 [33]. The uncertainty of the 2013 determination of k amounts, therefore, to 4.0 ppm. The value for k is not changed here because the effective areas determined in 2011 and 2015, see [33], respectively, agree well within the standard uncertainty estimate of the pressure measurement.

8. Interpolating DCGT

In the range from 4 K to 25 K, DCGT has been used for approximating the ITS-90 adopting the interpolation equation $T_{DCGT} = a + bp + cp^2$ prescribed in the text of the ITS-90 for constant-volume gas thermometry (CVGT) [41, 49]. The coefficients a, b, and c have been determined from the DCGT results by a calibration at the three required fixed points (vapour pressure of ^{4}He between 4.2 K and 5.0 K, triple points of hydrogen and neon). The approximation was done by deducing pressure values from the DCGT measurements for one selected relative change in capacitance γ, which corresponds nearly to a constant density of the thermometric gas ^{4}He. The deviation between two DCGT interpolations for densities of about 300 mol m^{-3} and 500 mol m^{-3} is negligible compared with the non-uniqueness of the ITS-90 [50]. The standard uncertainty of the interpolation with 500 mol m^{-3} ranges from 0.23 mK at 4.8 K to 0.29 mK at 25 K. These uncertainty estimates are supported by the results of the CIPM key comparison CCT-K1 'Realisations of the ITS-90, 0.65 K to 24.5561 K, using rhodium–iron resistance thermometers' [51] and by the comparison with a copy of a CVGT scale carried on resistance thermometers [41].

9. Conclusions and outlook

The principles, techniques and application fields of dielectric-constant gas thermometry are reviewed. Special emphasis is given to the influences responsible for the main components in the uncertainty budgets for various DCGT results. Four application fields are described in detail, namely primary and interpolating thermometry, the determination of the Boltzmann constant k at the triple point of water and the investigation of the thermophysical properties of the measuring gases helium, neon, and argon. The uncertainty of the already in [6] published value $k = 1.3806509 \times 10^{-23}\,J\,K^{-1}$ could be reduced to 4.0 ppm by reanalysing the component connected with the pressure measurement. Further progress is expected by using measuring capacitors of a quite different design, namely toroidal (ring) cross capacitors. This is important because it would be an independent check of the results based on cylindrical capacitors. Additionally, cross capacitors have several advantages like less sensitivity to dielectric films on the electrodes and an effective compressibility closer to that resulting from the volume compressibility of the electrode material. Considering the experience gained during the DCGT experiments at the TPW, it seems to be realistic to decrease the relative uncertainty of the Boltzmann constant to a level of only about (2–3) ppm, which would be sufficient for supporting the results of acoustic gas thermometry with respect to the new definition of the base unit kelvin by fixing the k value [52]. The experience gained in investigating thermophysical properties of gases (particle interaction, polarizability) applying DCGT will in future also be useful for getting data of technical gases (e.g. methane, hydrogen and their mixtures being important for energy storage) that are needed for establishing equations of state.

References

[1] Gugan D and Michel G W 1980 *Metrologia* **16** 149–67
[2] Gugan D 1991 *Metrologia* **28** 405–11
[3] Luther H *et al* 1996 *Metrologia* **33** 341–52

[4] Gaiser C and Fellmuth B 2009 *Metrologia* **46** 525–33
[5] Fellmuth B *et al* 2011 *Metrologia* **48** 1–9
[6] Gaiser C *et al* 2013 *Metrologia* **50** L7–11
[7] Gaiser C *et al* 2014 *Int. J. Thermophys.* **35** 395–404
[8] Fellmuth B *et al* 2006 *Meas. Sci. Technol.* **17** R145–59
[9] Smythe W R 1968 *Static and Dynamic Electricity* (New York: McGraw-Hill Book Company) pp 76–8
[10] Łach G *et al* 2004 *PRL* **92** 233001–4
[11] Puchalski M *et al* 2011 *Phys. Rev.* A **83** 042508
[12] Jentschura U D *et al* 2011 *Phys. Rev.* A **84** 064102
[13] Mohr P J *et al* 2012 *Rev. Mod. Phys.* **84** 1527–1605
[14] Gaiser C 2008 *Properties of Helium and Gas Thermometry* (Aachen: Shaker Verlag)
[15] Gaiser C *et al* 2010 *Int. J. Thermophys.* **31** 1428–37
[16] Gugan D 1982 *Temperature, Its Measurement and Control in Science and Industry* ed J F Schooley (New York: American Institute of Physics)
[17] Schmidt J W and Moldover M R 2003 *Int. J. Thermophys.* **24** 375–403
[18] Zandt T *et al* 2010 *Int. J. Thermophys.* **31** 1371–85
[19] Zandt T *et al* 2013 *AIP Conf. Proc.* **1552** 130–5
[20] Maynard J D 1992 *J. Acoust. Soc. Am.* **91** 1754–62
[21] Migliori A *et al* 1993 *Physica* B **183** 1–24
[22] Grüneisen E 1908 *Annalen der Physik* **26** 394–402
[23] Zandt T *et al* 2011 *Int. J. Thermophys.* **32** 1355–65
[24] Gaiser C *et al* 2008 *Int. J. Thermophys.* **29** 18–30
[25] Fellmuth B *et al* 2011 *IEEE Trans. Instrum. Meas.* **60** 2522–6
[26] Gaiser C *et al* 2007 Progress of Dielectric-Constant Gas Thermometry (DCGT) at PTB Report PTB-Th-3 (Braunschweig: PTB)
[27] Awan S *et al* 2011 *Coaxial Electrical Circuits for Interference-Free Measurements* (London: The Institution of Engineering and Technology)
[28] Sabuga W 2011 *PTB-Mitteilungen* **121** 247–55
[29] Sabuga W *et al* 2011 *PTB-Mitteilungen* **121** 256–9
[30] Sabuga W *et al* 2011 *PTB-Mitteilungen* **121** 260–2
[31] Priruenrom T 2011 *Development of Pressure Balances for Absolute Pressure Measurement in Gases up to 7 MPa* (Clausthal-Zellerfeld: Papierflieger Verlag)
[32] Sabuga W *et al* 2012 *Measurement* **45** 2464–8
[33] Zandt T *et al* 2015 *Metrologia* this special issue
[34] BIPM 1995 International electrotechnical commission (IEC), International federation of clinical chemistry (IFCC), International organization for standardization (ISO), International union of pure and applied chemistry (IUPAC), International union of pure and applied physics (IUPAP) and International organization of legal metrology (OIML) 1995 Guide to the expression of uncertainty in measurement (Geneva: International Organization for Standardization) ISO/IEC Guide 98
[35] Gaiser C and Fellmuth B 2010 *EPL* **90** 63002-p1–5
[36] Hall K R and Canfield F B 1967 *Physica* **33** 481–502
[37] Gaiser C *et al* 2015a *Metrologia*
[38] Fischer J *et al* 2011 *Int. J. Thermophys.* **32** 12–25
[39] Gaiser B *et al* 2015b *Phys. Status Solidi* to be published in
[40] Grüneisen E 1912 *Ann. Physik* **39** 257–306
[41] Fellmuth B *et al* 2005 Dielectric-constant gas thermometry and determination of the Boltzmann constant TEMPMEKO *2004, 9th Int. Symp. on Temperature and Thermal Measurements in Industry and Science* ed D Zvizdić *et al* (Zagreb: IMEKO / University of Zagreb)
[42] Beth E and Uhlenbeck G E 1937 *Physica* **4** 915–24
[43] Pais A and Uhlenbeck G E 1959 *Phys. Rev.* **116** 250–69
[44] White M P and Gugan D 1992 *Metrologia* **29** 37–57
[45] Berry K H 1979 *Metrologia* **15** 89–115
[46] Gaiser C and Fellmuth B 2008 *EPL* **83** 15001-p1-5
[47] Gaiser C *et al* 2015c *Int. J. Thermophys.* to be published in
[48] Gaiser C and Fellmuth B 2012 *Metrologia* **49** L4–L7
[49] Grohmann K *et al* 1996 Interpolating dielectric-constant gas thermometry *BIPM Com. Cons. Thermomètrie* **19** Document CCT/96-24
[50] Fellmuth B 2014 *Guide on the realization of the ITS-90: Introduction* (Sèvres: BIPM) (www.bipm.org/en/committees/cc/cct/guide-its90.html)
[51] Rusby R *et al* 2006 *Metrologia* **43** 03002
[52] Consultative Committee for Thermometry (CCT) 2014 *Recommendation T 1* (2014) On a new definition of the kelvin (Sèvres: BIPM) (www.bipm.org/cc/CCT/Allowed/Summary_reports/RECOMMENDATION_web_version.pdf)